

# Teleoperation through Brain Machine Interface

Achin Jain, Paras Ajay, Puneet Singhal, Sudipto Mukherjee  
Department of Mechanical Engineering  
Indian Institute of Technology Delhi  
New Delhi, India

**Abstract:** A brain machine interface (BMI) can be used to decode brain signals and control a robotic arm. The paper discusses its application as a prosthetic device, especially for spinal cord injury victims, suffering from paralysis. Neural data for experimentation is recorded from intra-cortical electrodes implanted in a macaque monkey at National Brain Research Center (NBRC). Brain signal decoding is achieved using the population vector algorithm (PVA). A delta manipulator with compliant linkages has been designed integrated with the BMI to perform a standard left-right instructed-delay centre-out reach task. An automatic raisin dispensing mechanism has also been designed and used to automate the complete experiment.

**Keywords**—Brain machine interface, neuroprosthesis, local field potential, population vector, delta manipulator, spinal injury

## I. INTRODUCTION

Motion signals emanating from the brain are transmitted to motor organs like legs and arms through very delicate neuronal pathways in the spinal cord. It is almost impossible to regenerate these nerve fibers once they are damaged. This is the fundamental reason why spinal cord injuries are so difficult to treat with conventional methods. In a revolutionary new approach, signals are tapped directly from a person's brain and decoded to obtain motion information. In this paper, we have tried to integrate some of the existing brain machine interfacing (BMI) technologies with an actual machine (a robotic manipulator).

The work presented here is especially relevant to spinal cord injury (SCI) victims who otherwise lead an exceedingly dependent life. Victims usually lose control of their motor functions, and in more extreme cases may also suffer from quadriplegia. Currently, patients have to undergo long and excruciating therapy sessions and still there is little hope of movement recovery. This paper demonstrates how a brain machine interface can be used to decode brain signals and control a robotic arm, which can be used as prosthesis.

An ideal Brain Machine Interface (BMI) or a neuroprosthesis consists of the following sub-processes implemented in real time: (1) Acquisition of movement signals directly from the disabled person's brain (2) Signal decoding to learn what kind of movement the person wants (3) Teleoperation of a highly dexterous robotic limb using the decoded information.

In this paper, all the three issues have been addressed but our work is primarily limited to (2) and (3). Further, all the three processes have been integrated into a single working setup.

Processed brain signals in the form of neural spikes are decoded using the Population Vector Algorithm. To simplify the overall BMI problem, instead of a highly dexterous robotic limb, a pick and place delta manipulator is designed as per the specifications and is controlled using a microcontroller. We conducted the experiments for only 1-D motion, i.e. left and right movement of the monkey's hand, since only this type of experiment was conducted at NBRC (from where brain signal data was taken). Another important task is to get the monkey to think of a particular movement direction. This requires a stimulus, which in our case is achieved by keeping raisins in different directions in front of the monkey. This further necessitates the development of a setup for automatic raisin dispensing.

The paper is organized as follows: in section II, the underlying principle behind the brain signal decoding has been explained. Following which, in the same section, the design of compliant delta manipulator and the automatic raisin dispensing mechanism used during the experimentation has been described. In section III, an overview of the integrated BMI is provided. A final discussion section concludes the paper.

## II. METHODOLOGY

### A. Data Description

Data sets were provided by Dr. Neeraj Jain's research group at National Brain Research Centre (NBRC). The data consists of signals from the pre-motor cortex of a macaque monkey.

The animal is seated on a primate chair with its non-performing arm and head restrained. The experimental setup allows the subjects to execute left or right reaching movements from a central location to one of two targets (where a raisin is placed as reward).

Brain signals are acquired using chronically implanted intra-cortical microelectrode arrays in the pre-motor cortex (specifically in the intra-parietal sulcus), while the primate executes standard left-right instructed-delay centre-out reach tasks. The signals are then sequentially passed through an amplifier, noise filter, spike detection and signal decoding algorithm.

### B. Timeline of a single trial

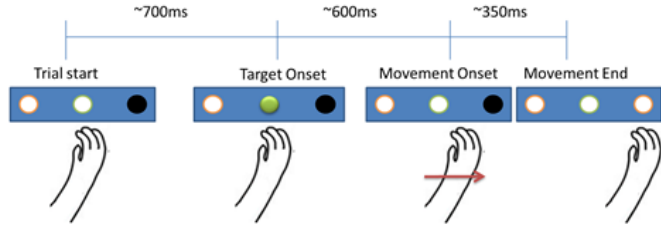


Figure 1: Single trial of a right reach task (black circle denotes the raisin which the monkey will pick): Trial starts when the monkey places its hand over the central circle. Target onset (green centre light) gives indication to begin motion. Movement onset is the act

Raw neural data is sampled at 140 kHz. In addition, sampling is done at 1000Hz frequency to capture the postsynaptic potentials.

### C. Signal Decoding: The Population Vector Algorithm

When individual neurons are represented as vectors that make weighted contributions along the axis of their preferred direction the resulting vector sum of all cell vectors (population vector) is in a direction congruent with the direction of movement [1]. Although, movement in three dimensions can be represented by population vectors (Todorov [2] has even correlated movement parameters like velocity using population vectors), a 1-D model has been used in our case.

The frequency of discharge of a particular neuron during movement in direction  $\{+\hat{i}, -\hat{i}\}$  has a linear relation:

$$d(M) = b + b_x m_x \quad \dots(1)$$

where  $b$  and  $b_x$  are the coefficients that vary from neuron to neuron and the values of these coefficients and their standard errors can be estimated using multiple regression techniques. The preferred direction for a particular neuron then is given by  $m_x$ . The movement direction is encoded in a unique fashion not by a single neuron but by an ensemble of neurons. The weight contribution,  $w_i(M)$ , of the  $i^{\text{th}}$  cell is a function of the movement direction and is taken to be equal to the change in cell activity from an offset level.

$$w_i(M) = d_i(M) - b_i \quad \dots(2)$$

Weighted vectorial contribution of the  $i^{\text{th}}$  cell is

$$N_i(M) = w_i(M) * C_i \quad \dots(3)$$

$C_i$  is the preferred direction of the  $i^{\text{th}}$  cell. The neuronal population vector  $P(M)$  corresponding to movement direction  $M$  is the sum of these cellular vectorial contributions

$$P(M) = \sum N_i(M) \quad \dots(4)$$

For our 1-D case, a positive  $P(M)$  would imply right movement and a negative  $P(M)$  would imply left movement.

### D. Delta Manipulator

A Delta manipulator consists of multiple kinematic chains connecting the base platform with the moving platform. The robot can also be seen as a spatial generalization of a four-bar linkage. The use of three parallelograms restrains rotational degrees of freedom of the moving platform. Hence, a delta robot has three pure translational dofs i.e. movement in the  $X$ ,  $Y$  or  $Z$  direction. The delta manipulator is widely used in industries for pick and place function. In this paper, this function is exploited for feeding raisins to the monkey during experimentation.

A cuboidal workspace ( $W$ ) is chosen for the delta robot. The dimensions of this cuboid are decided keeping in mind the actual movements that a monkey would make in the absence of a robot. In the figure 2,  $\Delta x = 0.2 m$ ,  $\Delta y = 0.4 m$ ,  $\Delta z = 0.25$ . Size of the monkey and the space availability for experimentation at NBRC were the major factors in deciding these parameters.

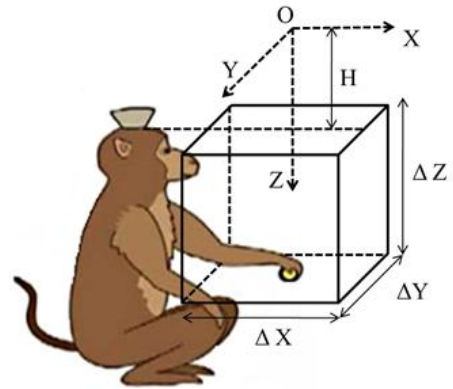


Figure 2: Workspace of the delta robot

Laribi [3] discusses a method to calculate link lengths of a delta manipulator. In his work, the kinematic relations are expressed in terms of the prescribed workspace of the robot. The same relations have been used while optimizing the geometric design variables ( $r_A$ ,  $r_B$ ,  $L_1$  and  $L_2$ ) of the manipulator.

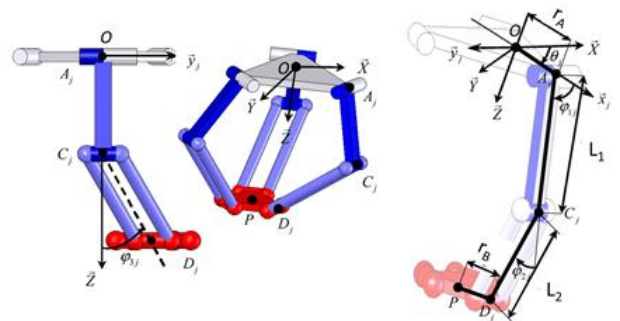


Figure 3 Geometry of Delta Robot [3]

$h_j$ , defining the boundary of the workspace, can be suitably expressed as:

$$h_j = ((X_p \cos(\theta_j) + Y_p \sin(\theta_j) - r)^2 + (X_p \cos(\theta_j) - Y_p \sin(\theta_j))^2 + (Z_p + H)^2 + L_2^2 - L_1^2)^2 - 4L_2^2 [(X_p \cos(\theta_j) + Y_p \sin(\theta_j) - r)^2 + (Z_p + H)^2] \leq 0 \quad \dots(5)$$

$h_j(X_p, Y_p, Z_p) = 0$  represents a torus. For 3 arms, we get 3 such equations. Our workspace should be confined within these 3 intersecting tori. Since W is a cuboid, delta workspace must include all the points P on and inside the cube. Minimizing the function  $|h_j(L_1, L_2, r_A, r_B, P)|$  with respect to the design variables, is equivalent to finding a surface closest to that point P. Here the desired volume is bounded by three surfaces ( $h_j$  where  $j=1,2,3$ ) and hence

$$F = \sum |h_1(L_1, L_2, r_A, r_B, P^k)| + \sum |h_2(L_1, L_2, r_A, r_B, P^k)| + \sum |h_3(L_1, L_2, r_A, r_B, P^k)| \quad \dots(6)$$

needs to be minimized.

Here,  $P^k$  refers to all the corner points of the cuboid with constraints:

$$L_1 \leq L_2 \text{ and } h_j(L_1, L_2, r_A, r_B, P^k) \leq 0 \quad j = 1,2,3 \text{ and } k = 1,2,3 \dots 8$$

This multidimensional nonlinear function is optimized using MATLAB Optimization Toolbox through an iterative process.

The end effector (figure 4) of the manipulator works on the principle of the camera shutter. It consists of 2 concentric rings (an inner rotating ring and an outer fixed ring), three flaps and an optional protective cover. Each flap has two pins, the outer one is constrained to move inside the slot provided in the outer ring while the inner pin goes into the corresponding hole in the inner ring. When the inner ring is driven by a servo motor the flaps rotate and the outer pin slides in its slot leading to opening of the end-effector aperture as shown in figure 5.



Figure 4: Exploded view of end effector

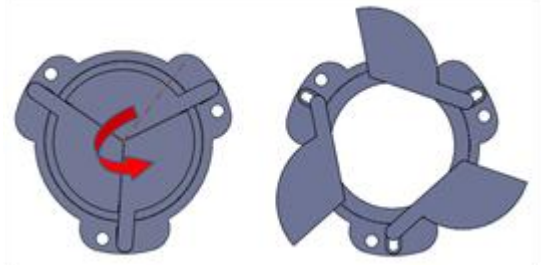


Figure 5: Anti-clockwise rotation of inner ring opens the shutter (right)

The manipulator uses compliant linkages. Utilizing the flexibility of these links, we avoided the use of complex joints. A single link can be modeled as a cantilever beam with constant cross section and linear material properties. Considering joint as fixed-pinned type, the analysis using elliptic integral theory shows that the free end follows a nearly circular path with the center of curvature lying on the undeflected length of the beam. The location of this pseudo rigid body's characteristic pivot is measured from the beam's end as a fraction of the beam's length. This fractional distance  $\gamma$  is found to be equal to 0.85 [4]. This principle can be extended to fixed-guided flexible segments as shown in figure 7. The deflection of the beam is anti-symmetric about the middle where the bending is zero. Thus, this can be analyzed as two cantilevers of half the length of the section with  $\gamma = 0.85$ .

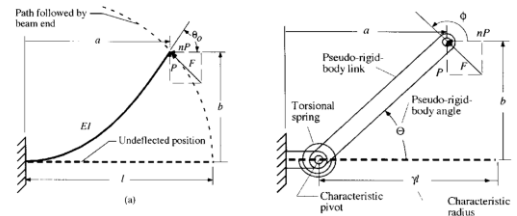


Figure 6: Deflection in cantilever beam and (b) Approximation of this bending by rotation about a pseudo joint

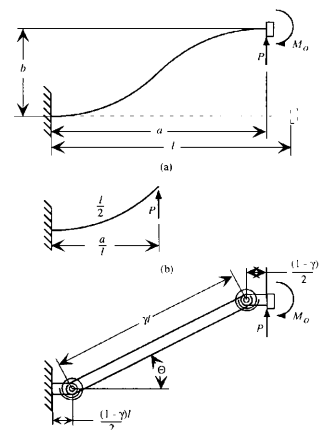


Figure 7: Fixed guided flexible segments

Further, the moment at the guided motion end is given by:

$$M_o = P l [1 - \gamma (1 - \cos \theta)] / 2 \quad \dots(7)$$

And joint stiffness or the spring constant is given by:

$$K = 2 \gamma K_\theta E I / l \quad \dots(8)$$

This value of stiffness is used while performing direct dynamics.

### E. Raisin Dispenser

The raisin dispenser can deliver raisins in a random manner to 8 different locations at some desired time without manual intervention. Automatic raisin dispensing is required since position variations during manual dispensing can affect the thought process of the monkey and thereby, alter the signals received.

Specifications:

- i. Maximum size of the raisin (length) : 10mm
- ii. Average time of a trial : 2-2.5s
- iii. Minimum number of trials in one session : 200
- iv. Maximum number of movement directions : 8
- v. Time between the target onset & the dropping of the raisin : 1.2-1.5s

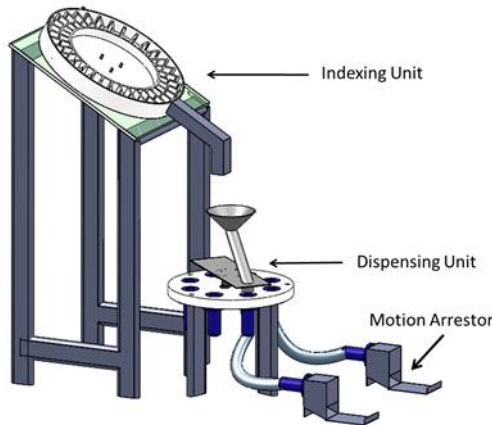


Figure 8: Raisin Dispensing Mechanism

One of the major problems with raisin dispensing during continuous trials is of raisin separation. To address this problem and also keeping in mind all the specifications, we came up with the design as shown in figure 9. The mechanism is broadly divided into two sub-assemblies, namely the indexing unit and the dispensing unit (figure 8).

The role of indexing unit is to keep the raisins separated from each other in small slots located on the periphery of a disc as shown in figure. Rotation of the indexing disc (disc with slots) is controlled by a servo motor and once a particular slot is at the lowest position of the disc, the contained raisin is discharged and carried to the dispensing unit through a square

channel. It rotates in steps equivalent to a slot size, every time a signal is sent at *Target Onset* during any trial (figure 1).

In the dispensing unit, the raisin is delivered to one of the 2 outlets using another servo controlled mechanism. The output is selected using Pseudo Random Number generator. Finally, the raisin, passing through one of the corresponding motion arrestors, slowly settles on a flat plate.

The indexing disc has 66 slots in total (2 rows of 33 each separated by concentric removable rings) filled to  $\frac{3}{4}$  of its capacity. Hence, the indexing unit can continuously dispense at most 2x25 raisins. To fulfill the requirement of 200 raisins, it was decided to use four such discs and incorporate a provision for easy detachment of the disc from the servo motor. Once the raisins are exhausted in the outer slots, inner ring (removable ring in figure 9) may be removed to make use of the next row of raisins. The outer ring ensures that raisin do not fall out while mounting the indexing disc on the motor.

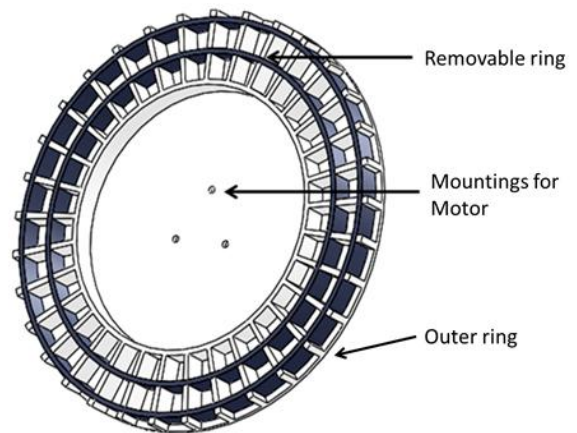


Figure 9: Indexing disc

### III. OVERVIEW OF THE BRAIN MACHINE INTERFACE SYSTEM

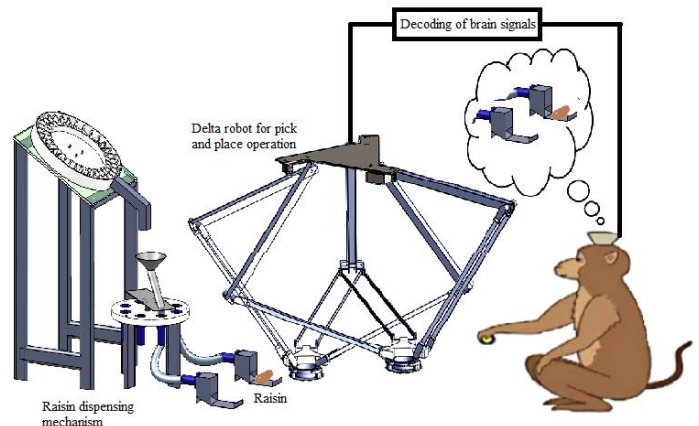


Figure 10: Teleoperation through BMI: A schematic

A trial begins with the automatic raisin dispensing mechanism dispensing a raisin to one of the left or right target positions in a random fashion. During real time

experimentation this would be the "Target onset" point. Since we are working only with offline data, at this point a pre-recorded left or right signal is sent to the decoding program (the program sending out the random brain signals acts as a virtual monkey). A population vector based decoding algorithm, which has been implemented by us, tells whether the selected signal corresponds to left or right hand movement. This decoded data is then sent to the delta robot controller, which executes a corresponding left or right motion.

MATLAB has been used for all programming and hardware interfacing tasks. A propeller servo controller has been used to control all the six servo motors used during experimentation.

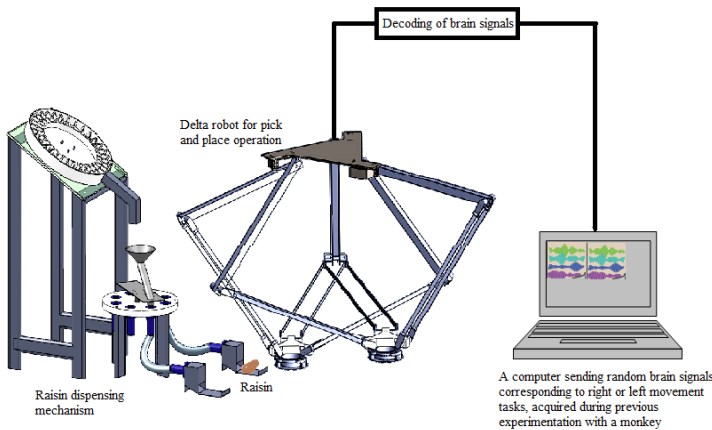


Figure 11: Final experimental setup

#### IV. DISCUSSION

The Population vector algorithm has been used for neural signal decoding. Data for 12 trials was obtained from NBRC of which 6 trials were used to find values of constants as discussed in section II C, while other 6 trials were used for testing (Table 1).

Correct decoding was achieved for all the direction selective neurons.

Table 1: P(M) values for four direction selective neurons while executing right and left hand movements

Trial number	Right movement Experiment	Left Movement Experiment
7	41.1	-50.3
8	44.8	-44.1
9	31.7	-63.9
10	33.3	-34.1
11	72.7	-58.2
12	69.8	-25.1

Although PVA has exceptional decoding capabilities, it has a serious drawback: signal decoding using PVA deteriorates significantly with electrode micro-motion (inevitably present during any long term application).

To overcome this difficulty some investigators [5] have used Common Spatial Patterns based decoding for post-synaptic neural activity (Local Field Potential). While this technique is not as reliable as PVA (Ranade G.[6] points out that as the low frequency component of intra-cortical recordings, the LFP is noisier than and not as effective as spike data when considered as direct input to a BMI), LFPs can serve as a supplementary source of signals for BMIs because of the fact that LFPs are additive signals derived and are consequently less prone to signal deterioration due to electrode micro-motion.

#### ACKNOWLEDGEMENT

We would like to thank Dr. Neeraj Jain (Professor) and Radhika Rajan (PhD. student) at National Brain Research Centre, Manesar for their valuable support in providing us with the experimental data. We would also thank Mr. D Jaitley at (Mechatronics Lab, IIT Delhi) for extending his continuous support towards realization of the project and Bhivraj Suthar (Research student, IIT Delhi) for helping us with the electronics.

#### REFERENCES

1. Georgopoulos A., Schwartz A., Kettner R., Neuronal Population Coding of Movement Direction, *Science* **233**, 1416 (1986)
2. Todorov E, "Direct cortical control of muscle activation in voluntary arm movements: A Model", *Nature Neuroscience*(2000) 3(4): 391-398
3. M.A. Laribi, L. Romdhane, S. Zegloul, "Analysis and dimensional synthesis of the DELTA robot for a prescribed workspace", *Mechanism and Machine Theory* 42 (2007) 859–870
4. L.L. Howell, "Compliant Mechanisms" Published by John Wiley & Sons, 2001
5. Ince Nuri F., Gupta Rahul, Arica Sami, Tewfik Ahmed H., Ashe James, Pellizzer Giuseppe, "Movement Direction Decoding with Spatial Patterns of Local Field Potentials", April 29 - May 2, 2009
6. Ranade G., "Information in the Local Field Potential: Implications for Brain Machine Interfaces"